AMERICAN SOCIETY FOR MICROBIOLOGY | Journal of Bacteriology®

RESEARCH ARTICLE

Arginine Biosynthesis Modulates Pyoverdine Production and Release in *Pseudomonas putida* as Part of the Mechanism of Adaptation to Oxidative Stress

Laura Barrientos-Moreno,[a] María Antonia Molina-Henares,[a] Marta Pastor-García,[a] María Isabel Ramos-González,[a] Manuel Espinosa-Urgel[a]

[a]Department of Environmental Protection, Estación Experimental del Zaidín, CSIC, Granada, Spain

ABSTRACT Iron is essential for most life forms. Under iron-limiting conditions, many bacteria produce and release siderophores—molecules with high affinity for iron—which are then transported into the cell in their iron-bound form, allowing incorporation of the metal into a wide range of cellular processes. However, free iron can also be a source of reactive oxygen species that cause DNA, protein, and lipid damage. Not surprisingly, iron capture is finely regulated and linked to oxidative-stress responses. Here, we provide evidence indicating that in the plant-beneficial bacterium *Pseudomonas putida* KT2440, the amino acid L-arginine is a metabolic connector between iron capture and oxidative stress. Mutants defective in arginine biosynthesis show reduced production and release of the siderophore pyoverdine and altered expression of certain pyoverdine-related genes, resulting in higher sensitivity to iron limitation. Although the amino acid is not part of the siderophore side chain, addition of exogenous L-arginine restores pyoverdine release in the mutants, and increased pyoverdine production is observed in the presence of polyamines (agmatine and spermidine), of which arginine is a precursor. Spermidine also has a protective role against hydrogen peroxide in *P. putida*, whereas defects in arginine and pyoverdine synthesis result in increased production of reactive oxygen species.

IMPORTANCE The results of this study show a previously unidentified connection between arginine metabolism, siderophore turnover, and oxidative stress in *Pseudomonas putida*. Although the precise molecular mechanisms involved have yet to be characterized in full detail, our data are consistent with a model in which arginine biosynthesis and the derived pathway leading to polyamine production function as a homeostasis mechanism that helps maintain the balance between iron uptake and oxidative-stress response systems.

KEYWORDS amino acid biosynthesis, iron acquisition, iron regulation, oxidative stress, siderophores

Iron plays an essential role in many cellular processes as a key element associated with proteins and enzymes participating in electron transport, energy metabolism, redox sensing, or DNA repair (1–4). Accordingly, the expression of numerous genes is regulated by iron availability in different microorganisms, and many bacteria display a battery of iron-sensing, iron uptake, and iron-scavenging mechanisms that often reflect their ecological niches and lifestyles (5–9). These mechanisms include the production and release of siderophores, a structurally diverse group of molecules, usually produced through nonribosomal peptide synthetases, that allow bacteria to efficiently acquire iron from the environment (reviewed in references 10 and 11). Siderophore production can influence bacterial fitness in environments as diverse as the rhizospheres of plants

Citation Barrientos-Moreno L, Molina-Henares MA, Pastor-García M, Ramos-González MI, Espinosa-Urgel M. 2019. Arginine biosynthesis modulates pyoverdine production and release in *Pseudomonas putida* as part of the mechanism of adaptation to oxidative stress. J Bacteriol 201:e00454-19. https://doi.org/10.1128/JB.00454-19.

Editor William W. Metcalf, University of Illinois at Urbana-Champaign

Address correspondence to Manuel Espinosa-Urgel, manuel.espinosa@eez.csic.es.

Received 5 July 2019
Accepted 22 August 2019
Accepted manuscript posted online 26 August 2019
Published 21 October 2019

(12) and the human gut (13) and has also been implicated in cross talk between bacterial species (14–16).

Despite its essential nature, excess free iron can have a detrimental effect on cell viability under aerobic conditions. It potentiates oxygen toxicity by causing an increase in hydroxyl ($^{\cdot}$OH) radicals through the Fenton reaction (17), in which hydrogen peroxide can react with ferrous iron, rendering $^{\cdot}$OH and OH^{-}. Further reactions of ferrous or ferric iron can also take place (17), causing an overall increase in reactive oxygen species (ROS), which then leads to lipid, protein, and DNA damage. Thus, it is not surprising that iron metabolism is not only tightly regulated but also coupled with the regulation of defense mechanisms against oxidative stress (18–20).

In the soil- and plant root-colonizing bacterium *Pseudomonas putida* KT2440, iron uptake has been shown to be relevant for attachment to corn seeds and bacterial fitness in the rhizosphere and in competition with other *Pseudomonas* species (21–23). Under iron-limiting conditions, the strain produces three forms of the siderophore pyoverdine, with slight structural differences (24). The most abundant form (PVD2) shows the following composition: succinamide-chromophore (2,3-diamino-6,7-dihydroxyquinoline)-Asp-ornithine-[hydroxyAsp-diaminobutanoic]-Gly-Ser-cyclohydroxyornithine, where the square brackets indicate a cyclic portion of the peptide chain. This portion is linear in the PVD1 variant, whereas the PVD3 variant contains succinic acid instead of succinamide (24).

Pyoverdine-mediated iron uptake is essential for surface motility of *P. putida* KT2440 (25) and has been described as a key factor involved in growth inhibition of the plant pathogen *Xanthomonas fragariae* by KT2440 (26). Increased siderophore production has been reported to take place during growth on the aromatic compound benzyl alcohol as a carbon and energy source (27). Besides an increase in pyoverdine production, iron limitation also results in changes in the metabolic flux and increased gluconate secretion during growth of *P. putida* KT2440 on glucose (28).

In a previous work, random transposon mutagenesis allowed the identification of the genes *argG* and *argH*, encoding the enzymes required for the last two steps of the arginine biosynthesis pathway (see Fig. S1 in the supplemental material), among a number of genetic elements involved in signaling mediated by the second messenger cyclic diguanylate (c-di-GMP) in *P. putida* KT2440 (29). c-di-GMP regulates the transition between motile and sessile lifestyles, biofilm development, and other cellular processes in a large number of bacterial species (recently reviewed in reference 30).

In the course of their characterization, we observed that mutants in *argG* and *argH* exhibited changes in the color of colonies and liquid cultures, as well as reduced fluorescence, suggestive of altered siderophore production (Fig. 1A). These observations prompted us to explore the connection between arginine biosynthesis and pyoverdine production, which is presented in this work.

RESULTS

Arginine auxotrophy causes reduced pyoverdine release and increased sensitivity to iron depletion. As an initial step to establish the potential link between arginine and pyoverdine synthesis, null mutants in *argG* and *argH* were constructed by deletion of the complete open reading frames (PP_1088 and PP_0184, respectively). These mutants, which are auxotrophs for arginine but grow normally in King's B medium (see Fig. S2 in the supplemental material), exhibited reduced fluorescence under UV light with respect to the wild type after overnight growth in liquid King's B medium (Fig. 1A), a phenotype similar to that of a mutant in *pvdD* (PP_4219; previously annotated as *ppsD*), which does not produce pyoverdine (25) and was used as a negative control. Addition of 5 mM L-arginine to the growth medium restored fluorescence in the Δ*argG* and Δ*argH* mutants (Fig. 1A).

Further analysis of siderophore production was done by a chrome azurol S (CAS) assay (Fig. 1B). The Δ*argG* and Δ*argH* mutants grew normally, but the characteristic yellow-orange halo indicative of pyoverdine diffusion into CAS medium was nearly absent, in contrast with the wild-type strain. This defect was restored by addition of

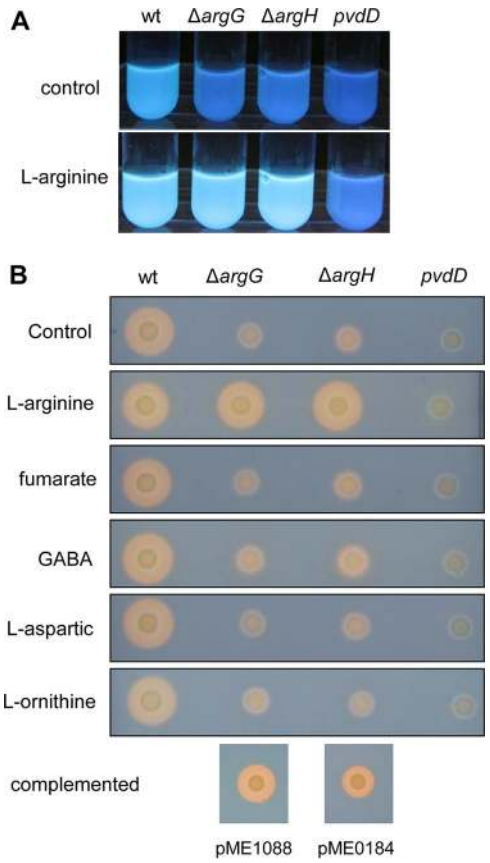

FIG 1 Analysis of pyoverdine production and release in KT2440, Δ*argG*, Δ*argH*, and *pvdD* (negative-control) strains. (A) Fluorescence detection in liquid cultures grown in King's B medium in the absence (control) or presence of 5 mM L-arginine. wt, wild type. (B) CAS assay detection of pyoverdine release (orange halo) in the absence or presence of different compounds related to arginine metabolism added at a final concentration of 5 mM. The Δ*argG* and Δ*argH* mutants complemented with plasmids carrying each wild-type gene (pME1088 and pME0184, respectively) were also included. Experiments were repeated three times, with three replicates each; representative images are shown. GABA, gamma-aminobutyric acid.

5 mM L-arginine to the growth medium, as well as by complementing the mutations with plasmids pME1088 and pME0184, bearing the wild-type loci (29). Addition of fumarate (also produced in the last step of arginine biosynthesis) or gamma-aminobutyrate (one of the main metabolites into which different arginine catabolism routes converge) did not restore the appearance of the pyoverdine halo in either mutant (Fig. 1B). Interestingly, neither did L-ornithine or L-aspartic acid, both of which are structural components of pyoverdine (Fig. 1B) and substrates in arginine synthesis (see Fig. S1).

Pyoverdine production was further analyzed in several mutants affected in different steps of the arginine biosynthetic route. As indicated in Fig. 2, mutations in *argA*, *argB*, and *argF* caused essentially the same reduction in pyoverdine release as the *argG* and *argH* mutations, and halo production was restored to different extents by addition of 5 mM L-arginine. Interestingly, mutations affecting *argD*, *argE*, and *argJ* resulted in either no change or a minor decrease in the halo area. It should be noted that these three mutants do not display arginine auxotrophy, unlike the rest of the mutants tested, which are unable to grow in minimal medium in the absence of exogenous arginine (see Fig. S2).

Although *P. putida* KT2440 has a range of other iron complex uptake mechanisms, the observed reduction in siderophore production might be expected to result in less efficient iron uptake by the arginine biosynthesis mutants. To check if this was the case, inductively coupled plasma-optical emission spectrometry (ICP-OES) was used to de-

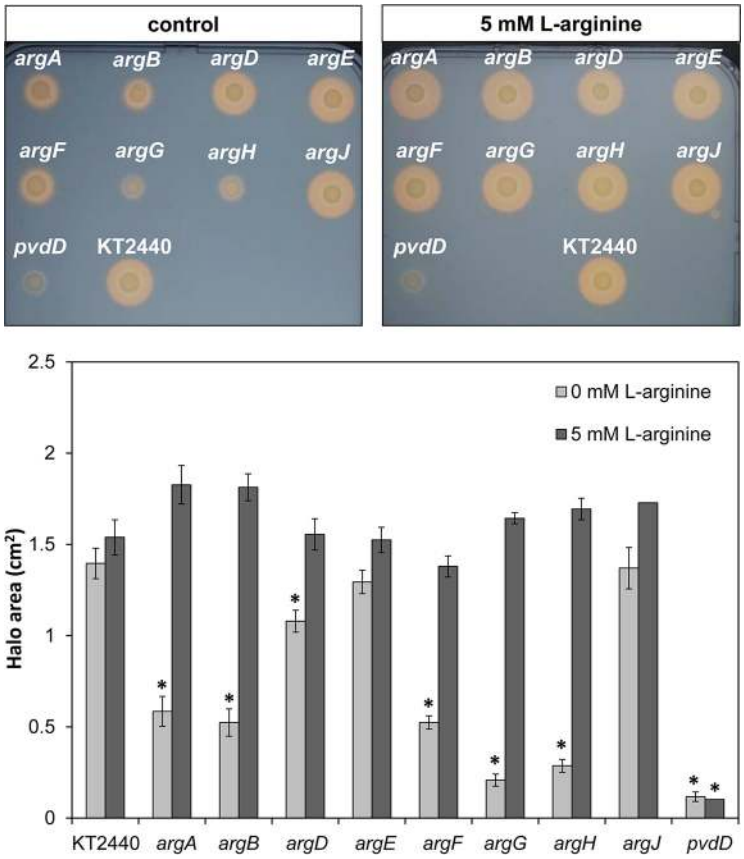

FIG 2 Analysis of pyoverdine production and release in different mutants in the arginine biosynthesis pathway. CAS assays similar to those shown in Fig. 1 were performed in the presence or absence of 5 mM L-arginine (top), and the area of the halo produced by each strain was calculated after subtracting the area covered by the culture growth patch (bottom). The data correspond to averages and standard deviations from three independent experiments with three replicates each. Statistically significant differences from the wild type are indicated by asterisks (Student's *t* test; $P < 0.05$).

termine the concentration of iron remaining in the supernatants of cultures after overnight growth in King's B medium, as described in Materials and Methods. As shown in Fig. 3A, the relative amount of iron that had not been incorporated into the cells was higher in the *argG* and *argH* mutants than in the wild type, as was the case for the *pvdD* mutant.

Bacterial strains that are defective or limited in iron uptake are generally sensitive to nonmetabolizable iron chelators (22, 23). We therefore decided to compare the growth of the Δ*argG* and Δ*argH* mutants with that of the wild type in the presence of increasing concentrations of 2,2′-bipyridyl. The results presented in Fig. 3B show that growth of both mutants was impaired at chelator concentrations above 1.3 to 1.5 mM, whereas the parental strain was able to grow at higher concentrations of 2,2′-bipyridyl.

Expression of some pyoverdine-related genes is altered in Δ*argG* and Δ*argH* mutants. One possibility to explain the results described above could be that expression of pyoverdine-related genes was altered in the arginine auxotrophs. Several genes involved in pyoverdine synthesis, transport, and regulation (their genetic context is shown in Fig. S3 in the supplemental material) were selected to analyze their mRNA levels in the Δ*argG* and Δ*argH* mutants compared to the parental strain by quantitative real-time PCR (qRT-PCR) after growth in King's B medium. The genes analyzed were *pvdD* and *pvdA*, encoding a pyoverdine nonribosomal peptide synthetase and a protein involved in pyoverdine side chain synthesis, respectively (31); *pvdE*, encoding an ATP-binding membrane protein presumably required for pyoverdine translocation to the periplasm (32, 33); *pvdP*, which encodes a tyrosinase involved in chromophore

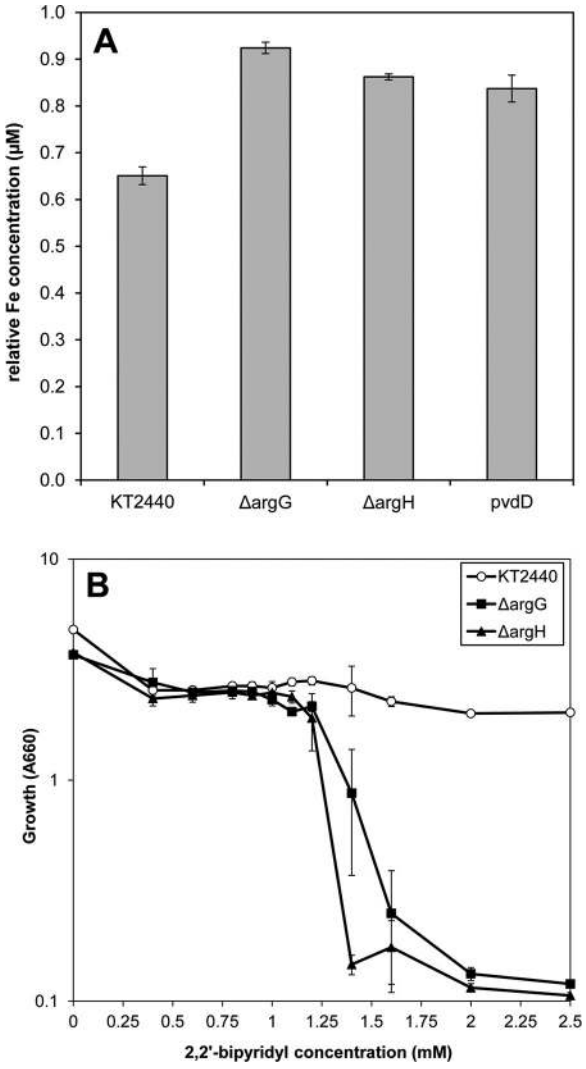

FIG 3 (A) Quantification of residual iron in King's B medium after overnight growth of cultures of KT2440, Δ*argG*, Δ*argH*, and *pvdD* strains. The data were corrected for growth (OD_{660}), and average relative values and standard deviations are presented, corresponding to two biological replicates with three technical replicates each. Differences between the wild type and the three mutants were statistically significant (Student's *t* test; $P < 0.01$). (B) Effect of iron chelation on growth of KT2440 and the Δ*argG* and Δ*argH* mutants. Cultures were inoculated at an initial OD_{660} of 0.05 in liquid LB medium with increasing concentrations of 2,2′-bipyridyl, in duplicate. Growth was analyzed after 24 h by measuring the turbidity (OD_{660}) of the cultures. The data correspond to averages and standard deviations of three independent experiments.

maturation (34); and two regulatory genes, *pvdS*, encoding an alternative sigma factor whose homologue in *Pseudomonas aeruginosa* constitutes the master transcriptional regulator for pyoverdine synthesis and transport (35, 36), and *algQ* (named *pfrA* in *Pseudomonas fluorescens* [37]), which has been reported to sequester the housekeeping sigma factor σ^{70} to allow increased availability of RNA polymerase for PvdS binding (38).

The results of the qRT-PCR analysis are shown in Fig. 4. Intriguingly, both the Δ*argG* and Δ*argH* mutants showed increased (between 3- and 5-fold) expression of the pyoverdine structural genes *pvdA* and *pvdD* with respect to the wild type, whereas expression of *pvdE* was reduced (around −2.5-fold). Expression of *pvdP* and the regulatory genes *pvdS* and *algQ*, on the other hand, did not show significant changes in the mutants with respect to the wild type.

Arginine biosynthesis mutants retain pyoverdine intracellularly. The expression data suggested that the differences observed in the CAS assays and in liquid cultures

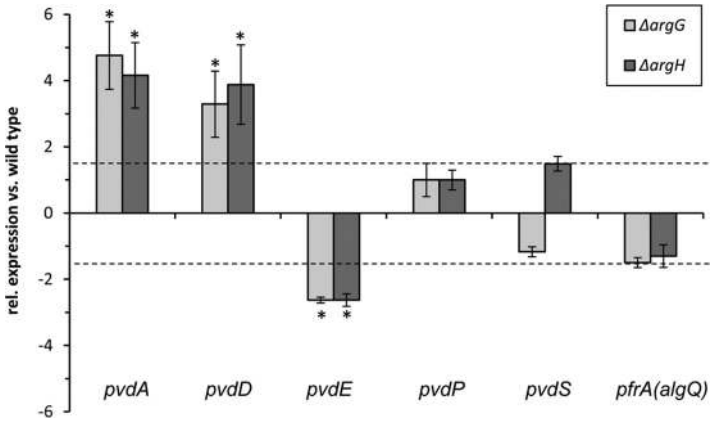

FIG 4 Expression levels of pyoverdine-related genes in Δ*argG* and Δ*argH* mutants with respect to the wild type, analyzed by qRT-PCR after growth in King's B medium. The data are averages and standard deviations from three biological replicates with three technical replicates each. The asterisks indicate relevant changes based on statistically significant differences from the wild type (Student's *t* test; $P < 0.05$) and considering a ± 1.5-fold change as the cutoff value (dashed lines).

were not simply due to limited pyoverdine synthesis, which could actually be increased in the Δ*argG* and Δ*argH* mutants, but rather to reduced transport of the siderophore to the periplasm for its full maturation and further release from bacterial cells. To confirm this idea, extracellular and intracellular pyoverdine were separately quantified, as described in Materials and Methods, in overnight cultures of the Δ*argG* and Δ*argH* mutants, with wild-type KT2440 and the *pvdD* mutant as positive and negative controls, respectively (Fig. 5A). Both the Δ*argG* and the Δ*argH* mutants displayed reduced fluorescence in the culture supernatant, whereas it was increased in disrupted cells. These data indicate that although the mutants produce less mature pyoverdine, a larger proportion of it is retained inside the cells (around 5% is retained in the wild type, whereas between 40 and 20% is retained in the *argG* and *argH* mutants, respectively).

Further support for this result was obtained through observation of cells by fluorescence microscopy (see Fig. S4 in the supplemental material): the parental strain showed intense fluorescence, background and around the perimeters of the cells, indicative of pyoverdine maturation in the periplasm and release into the medium. Background and cell fluorescence was significantly less intense in the Δ*argG* and Δ*argH* mutants, although heterogeneity was observed among the cells, with many of them showing uniform fluorescence while in others fluorescence was more evident in the perimeter.

One potential explanation for these results is that the *argG* and *argH* mutants are defective in sensing reduced iron availability. To test this possibility, intracellular and extracellular pyoverdine were quantified in cultures grown under further iron-limiting conditions by adding a subinhibitory concentration (200 μM) of the iron chelator 2,2′-bipyridyl. As shown in Fig. 5B, under these conditions, there was an increase in extracellular pyoverdine in both mutants. Although the values were still below those of the wild type, the relative increase was higher in the mutants (4- to 6-fold) than in the parental strain (around 2.5-fold).

Some polyamines promote pyoverdine release and alleviate oxidative stress. As mentioned in the introduction, despite its essential nature, free iron enhances oxidative damage in cells. Several reports have indicated that polyamines can have a protective function against oxidative stress (39, 40). Since arginine is the main precursor of polyamine synthesis (see Fig. S5 in the supplemental material), we hypothesized that limited pyoverdine release in the arginine biosynthesis mutants might reflect the existence of a balancing mechanism between oxidative-stress protection and fulfilling cellular iron requirements. Thus, under conditions in which arginine availability is limited or polyamine synthesis is disfavored, iron entry into cells would be reduced and/or

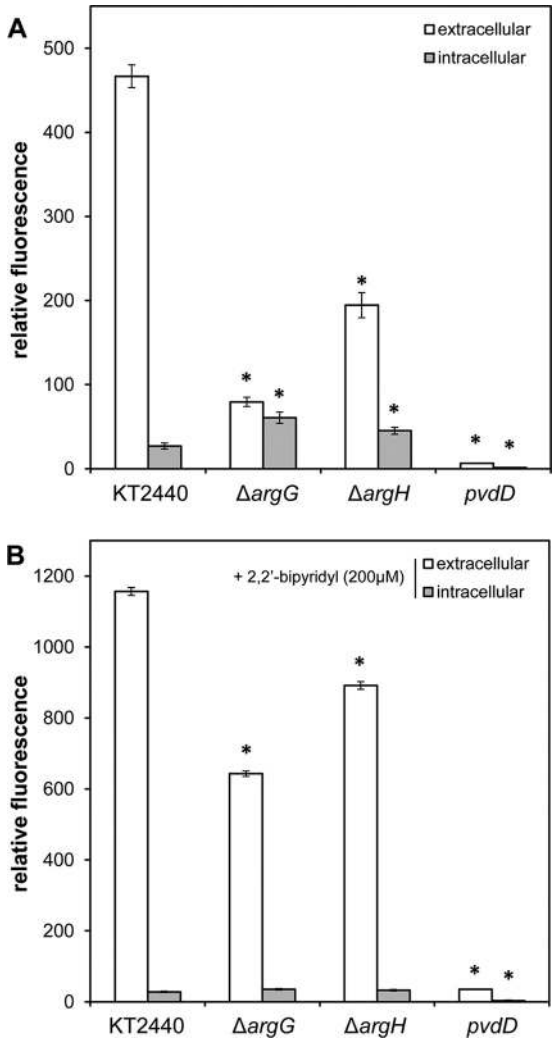

FIG 5 Quantification of extracellular and intracellular pyoverdine fractions in liquid cultures grown in King's B medium in the absence (A) or presence (B) of 200 μM 2,2′-bipyridyl. Fluorescence was measured using a Varioskan Lux microplate reader by recording emission at 455 nm upon excitation at 398 nm. Fluorescence readings were corrected for growth (OD_{660}), and average relative values and standard deviations are presented, corresponding to three biological replicates with three technical replicates each. Statistically significant differences with respect to the corresponding value in the wild type are indicated by asterisks (Student's *t* test; $P < 0.01$).

pyoverdine would be retained to aid in intracellular iron sequestration. If this hypothesis were correct, it would be expected that addition of exogenous polyamines would result in higher tolerance for oxidative stress, along with increased pyoverdine release. We therefore decided to check if polyamines had an effect similar to that of arginine in terms of pyoverdine production. As shown in Fig. 6, addition of 5 mM agmatine or spermidine caused a significant increase in pyoverdine production in KT2440 and to a lesser extent in the *argG* and *argH* mutants. Intriguingly, putrescine had no clear effect in any of the strains. These results are not likely to be a consequence of polyamine metabolism being able to reestablish cellular arginine pools, since spermidine supplementation did not restore growth of the mutants in minimal medium in the absence of arginine (data not shown).

We next tested if oxidative stress might be alleviated by exogenously added polyamines. For that purpose, exponentially growing cultures of KT2440, with or without spermidine supplementation (5 mM), were exposed to 5 mM H_2O_2, and further growth was monitored over several hours. The results presented in Fig. 7 show that

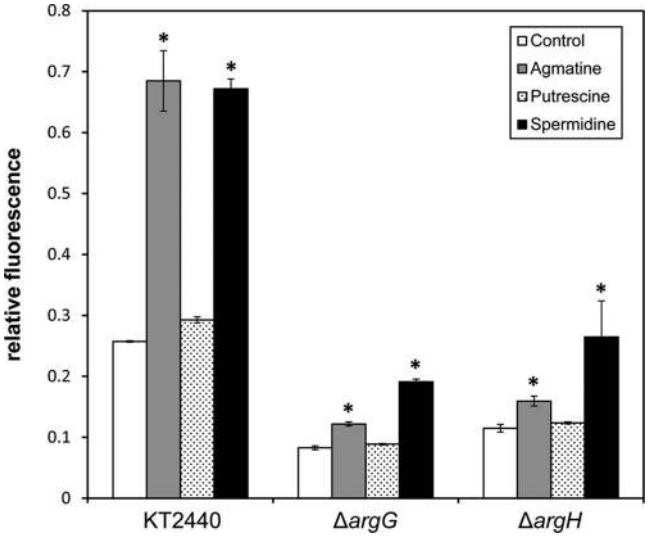

FIG 6 Quantification of fluorescence resulting from extracellular pyoverdine in KT2440 and the Δ*argG* and Δ*argH* mutants after 24 h of growth in King's B medium supplemented with different polyamines, using a Varioskan Lux fluorimeter. Fluorescence readings were normalized for growth (OD_{660}). Average relative values and standard deviations are presented, corresponding to three biological replicates with three technical replicates each. The asterisks indicate statistically significant differences from the control without addition (Student's *t* test; $P < 0.01$).

addition of the stressor caused complete growth arrest in the absence of spermidine for at least 3 h. Spermidine supplementation nearly abolished this inhibitory effect, even though the presence of spermidine reduced the growth rate of KT2440. This reduction may derive from the detrimental effect of spermidine on protein synthesis, reported in other bacteria (41, 42).

The above-described results made us explore further the possible interplay between arginine biosynthesis, pyoverdine, and oxidative stress. Thus, if the siderophore did play a role in oxidative-stress tolerance, a pyoverdine-deficient mutant should show increased ROS production. The same would be expected for the *argG* and *argH* mutants, where polyamine synthesis would be hampered. To test this, cultures of KT2440 and

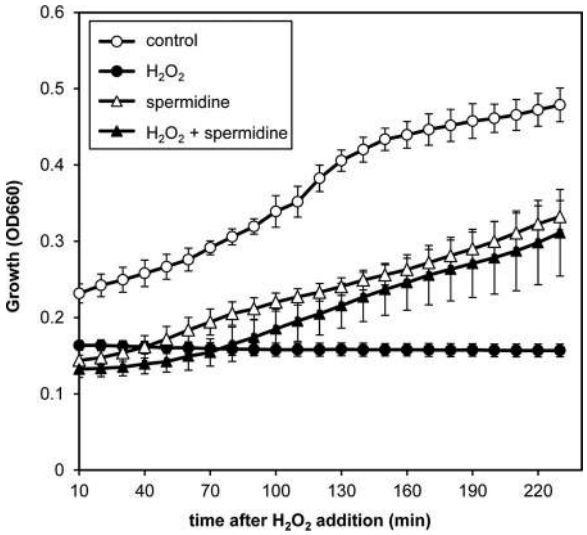

FIG 7 Growth of *P. putida* KT2440 in the absence (open symbols) and presence (closed symbols) of 5 mM H_2O_2, without (circles) or with (triangles) 5 mM spermidine. Cultures were grown as described in Materials and Methods. The results are averages and standard errors from two independent assays with 4 replicates.

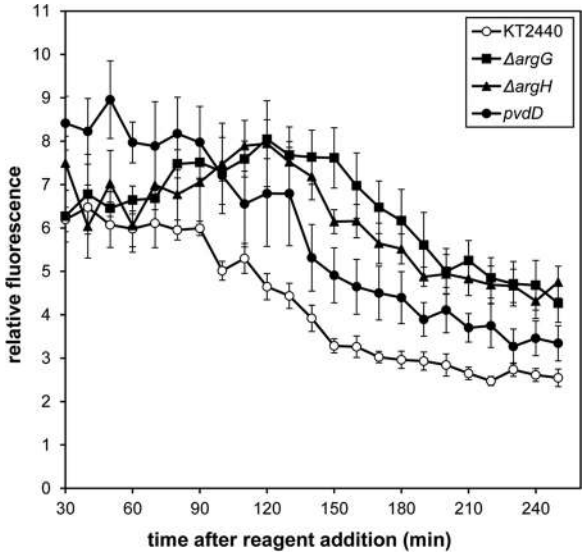

FIG 8 Fluorescence-based measurement of reactive oxygen species in KT2440 and the *pvdD*, Δ*argG*, and Δ*argH* mutants, using CellROX Deep Red reagent. The data correspond to fluorescence readings normalized with respect to the OD_{660} at each time point and are the averages and standard errors from two independent assays with 6 replicates.

the *argG*, *argH*, and *pvdD* mutants were exposed to CellROX Deep Red reagent (Life Technologies), a fluorogenic sensor for ROS, and fluorescence was followed during growth, as detailed in Materials and Methods. The three mutants showed higher fluorescence than the wild-type strain (Fig. 8), indicating increased ROS production or reduced detoxification.

DISCUSSION

In this work, we have exposed the connection between arginine metabolism and pyoverdine, a siderophore with high affinity for iron. Mutants deficient in arginine synthesis are also deficient in the production of mature extracellular siderophore, a defect that is restored by addition of the amino acid to the culture medium. It is worth noting that not all the mutations in the genes that encode enzymes of the arginine biosynthesis pathway lead to auxotrophy for the amino acid. Particularly interesting was the fact that an *argD* mutant was still able to grow in the absence of arginine, indicating that another transaminase can participate in the conversion of *N*-acetyl-glutamate semialdehyde into *N*-acetyl ornithine, thus compensating for the defect in *argD*. Such promiscuity has been previously reported in other transaminases (43), and it is not uncommon for *P. putida* to have redundant or promiscuous enzymes involved in metabolism (44).

Arginine is a constituent of the peptide chain of type 1 pyoverdine in *P. aeruginosa* (45). However, the siderophore produced by *P. putida* KT2440 does not include the amino acid in its structure (24), and the same has been predicted for other *P. putida* strains (46). Thus, altered production of pyoverdine in the arginine-auxotrophic mutants is not due to limitation in one of its building blocks, and neither is it restored by addition of other compounds, such as L-aspartic acid or L-ornithine, which are intermediaries in the arginine biosynthesis pathway, can be efficiently transported into the cell and used as carbon and nitrogen sources, and are structural constituents of the siderophore. While we cannot exclude the possibility that altered metabolic fluxes resulting from these mutations influence pyoverdine synthesis, our data are compatible with other possibilities. In fact, the Δ*argG* and Δ*argH* mutants do produce pyoverdine and even show increased expression of the pyoverdine structural genes *pvdD* and *pvdA* with respect to the wild-type strain, but the total amount of mature siderophore is smaller, and it is in part retained within the cell and not released into the extracellular

medium. This is consistent with the reduced expression of *pvdE* in both mutants. PvdE has been reported to transport immature pyoverdine across the inner membrane into the periplasm, where full maturation of the molecule takes place (33). The Δ*argG* and Δ*argH* mutants would therefore show inefficient transport and maturation of the siderophore. The precise mechanisms underlying these alterations have yet to be fully characterized. They are not associated with relevant changes in the expression of the regulatory gene *pvdS* or *algQ* or with the mutants being insensitive to iron deprivation, since addition of an iron chelator increases their production and release of siderophore.

Our data also suggest that mature pyoverdine can be present in the cytosol and might function along with other proteins, such as bacterioferritins, as an additional iron scavenger. In this respect, it is worth mentioning that pyoverdine has been reported to efficiently bind and oxidize ferrous iron (47), the form responsible for the Fenton reaction leading to ROS production. Hence, our hypothesis was that the retention of pyoverdine in these mutants could reflect the existence of a balancing mechanism that connects iron uptake and oxidative stress, and we postulate that polyamines participate in it, considering that the lack of arginine synthesis would result in reduced synthesis of polyamines. These molecules are involved in different relevant physiological processes, including biofilm formation, symbiosis, and virulence mechanisms, and have been reported to play a protective role against ROS in different organisms (40, 48). It is worth mentioning that connections have previously been established between polyamines, iron, and stress: polyamine synthesis and transport genes have been identified in *P. aeruginosa* as part of the BqsR regulon (20). The BqsS/BqsR two-component signal transduction system responds to ferrous iron and has been implicated in the adaptation and stress response of *P. aeruginosa* to the conditions found during lung colonization.

Consistent with our hypothesis, a pyoverdine-deficient mutant showed increased production of reactive oxygen species (which are involved in oxidative damage, although they can also play a signaling role) with respect to the wild type, and the same was observed with the arginine biosynthesis mutants, which are presumably hampered in polyamine synthesis. Furthermore, the presence of certain polyamines in the growth medium can reduce oxidative stress and promote pyoverdine release. The fact that spermidine and agmatine, but not putrescine, had this stimulatory effect on pyoverdine release is intriguing and will require further analysis. It may result from different transport efficiencies for each polyamine, or it could be related to the structural differences between the molecules; the additional NH group in agmatine and spermidine, absent in putrescine, might hold the clue. Our data, summarized in Fig. 9, indicate that the arginine/polyamine biosynthesis pathway functions as a homeostasis device responsible for maintaining the equilibrium between iron uptake and oxidative-stress responses in *P. putida*. Further work will be required to fully reveal the underlying molecular mechanisms and to determine if similar connections are present in other bacteria with different environmental lifestyles, particularly in species such as *P. aeruginosa*, where iron metabolism and regulation are much better known.

MATERIALS AND METHODS

Bacterial strains, culture media, and growth conditions. The strains and plasmids used in this work are listed in Table 1. *P. putida* KT2440 (49) and its derivatives were routinely grown at 30°C and *Escherichia coli* strains at 37°C in LB medium (50). Alternatively, M9 minimal medium supplemented with trace metals (51) and glucose or citrate as a carbon source was used. King's B medium was used to analyze pyoverdine production (52). When appropriate, antibiotics were used at the following concentrations (micrograms per milliliter): chloramphenicol (Cm), 30; kanamycin (Km), 25; rifampin, 10; piperacillin (Pip), 30; ampicillin (Ap), 100; streptomycin (Sm), 50 (for *E. coli*) or 100 (for *P. putida*); nitrofurantoin (Nit), 100. Amino acids and other reagents (Sigma-Aldrich and Fluka Chemicals) were added at the indicated concentrations in each case.

Molecular biology techniques. DNA preparation, digestion with restriction enzymes, plasmid dephosphorylation, ligation, and cell transformations were done using standard protocols (53, 54). Plasmid purification and DNA extraction from agarose gels (NZY Tech and Qiagen kits, respectively) were carried out following the manufacturers' instructions. A digoxigenin (DIG)-DNA labeling and detection kit (Roche) was used for Southern hybridization as recommended by the manufacturer.

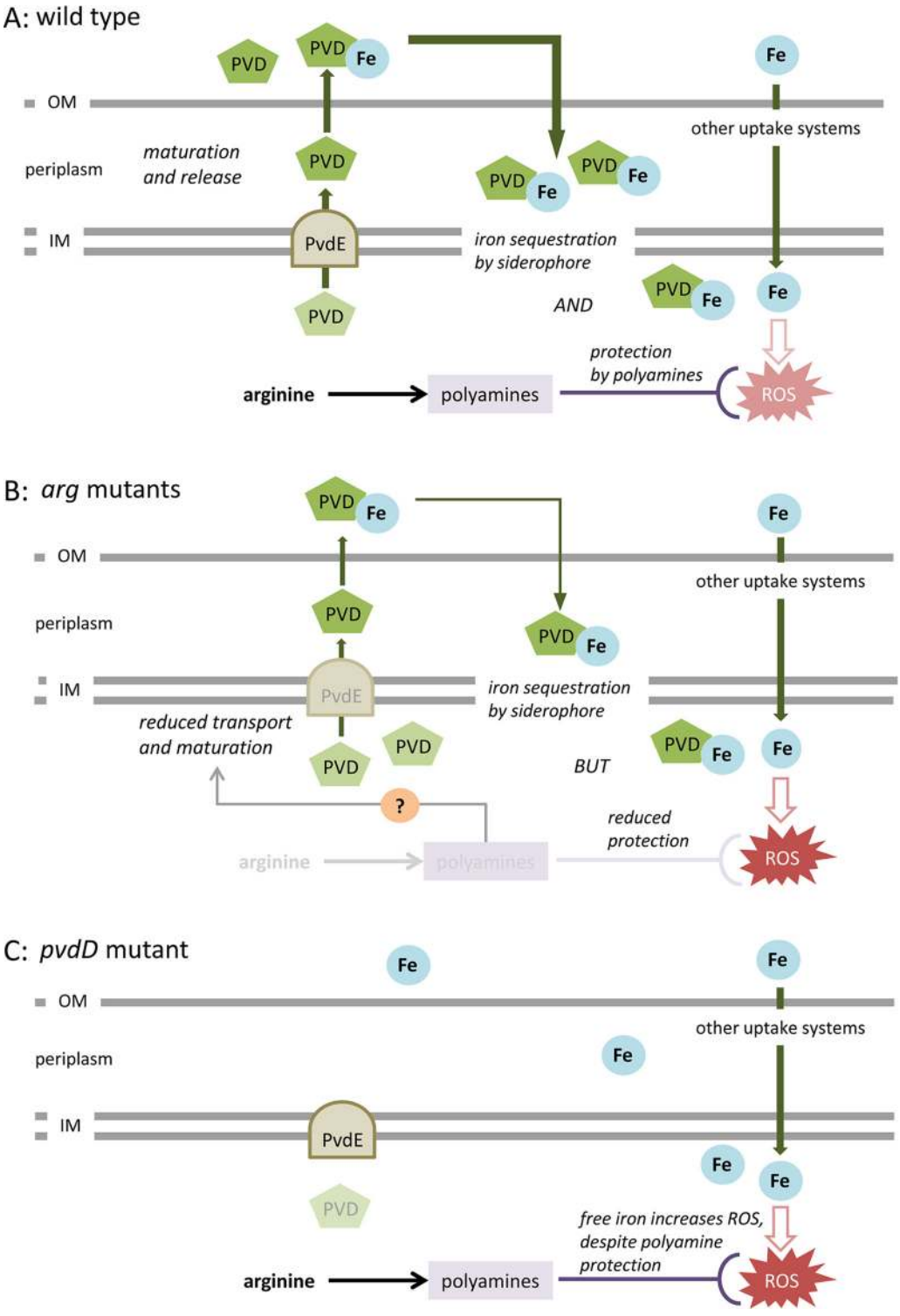

FIG 9 Schematic summary of the proposed connections between arginine/polyamines, iron uptake, and oxidative stress. (A) In the wild-type strain, low iron activates pyoverdine (PVD) production and maturation (dark-green pentagons) to restore intracellular iron pools. The siderophore sequesters extracellular and intracellular iron, while polyamines protect against ROS that can derive from iron chemistry. (B) When polyamine production is disfavored, such as in the arginine biosynthesis mutants, protection against ROS is hampered. This leads to reduced pyoverdine release and therefore limited iron capture, as a proposed mechanism to control intracellular free iron and minimize ROS production. (C) In a pyoverdine-deficient mutant, polyamine synthesis would be intact but insufficient for full protection against ROS due to the lack of siderophore available to sequester free iron.

TABLE 1 Strains and plasmids used in this work

Strain or plasmid	Relevant features[a]	Reference or source[b]
P. putida		
KT2440	Wild-type strain; mt-2 derivative cured of pWW0	49
Δ*argG* strain	Null mutant in *argG* (PP_1088); complete deletion	This work
Δ*argH* strain	Null mutant in *argH* (PP_0184), complete deletion	This work
Δ*argF* strain	Null mutant in *argF* (PP_1079), complete deletion	This work
argJ::Km strain	Km^r; mini-Tn*5* transposon insertion mutant in *argJ* (PP_1346)	PRCC
argA::Km strain	Km^r; mini-Tn*5* transposon insertion mutant in *argA* (PP_5185)	PRCC
argB::Km strain	Km^r; mini-Tn*5* transposon insertion mutant in *argB* (PP_5289)	PRCC
argD::Km strain	Km^r; mini-Tn*5* transposon insertion mutant in *argD* (=*astC* [PP_4481])	PRCC
argE::Km strain	Km^r; pCHESI-Ω-Km insertion mutant in *argE* (PP_5186)	PRCC
pvdD::Km strain	Km^r; mini-Tn*5* transposon insertion mutant in *pvdD* (PP_4219)	25
E. coli		
DH5α	*supE44 lacU169* (ϕ80*lacZ*ΔM15) *hsdR17* (r_K^- m_K^-) *recA1 endA1 gyrA96 thi-1 relA1*; cloning host	56
CC118λ*pir*	Rif^r λ*pir* for stable maintenance of pKNG101 derivatives	55
HB101(pRK600)	Cm^r *mob tra*; helper strain for triparental conjugation	55
Plasmids		
pCR2.1 TOPO	Km^r; cloning vector for PCR products	Invitrogen
pKNG101	Sm^r *oriR6K mobRK2 sacBR*	57
pME1088	Ap^r Pip^r; *argG* open reading frame cloned in pMMB67HE	29
pME0184	Ap^r Pip^r; *argH* open reading frame cloned in pMMB67HE	29

[a]Rif, rifampin; Cm, chloramphenicol; Km, kanamycin; Sm, streptomycin; Pip, piperacillin; Ap, ampicillin.
[b]PRCC, *Pseudomonas* Reference Culture Collection (http://artemisa.eez.csic.es/prcc/).

Triparental conjugation. Transfer of plasmids from *E. coli* to *P. putida* strains was performed by triparental mating using *E. coli*(pRK600) as a helper, as previously described (55). For each strain, 0.5 ml of overnight cultures grown in LB medium was collected by centrifugation, resuspended in 50 μl of fresh LB medium after several washing steps, and spotted on a nitrocellulose filter (0.22-μm pore diameter) on LB agar plates, which were incubated overnight at 30°C. Then, the cells were scraped off the mating filter and resuspended in 1.5 ml of diluted M9 salts medium. Serial dilutions were plated on selective LB medium supplemented with the appropriate antibiotics to select exconjugants and counterselect donor, helper, and recipient strains.

Generation of null mutants. Null mutants were generated by gene replacement via homologous recombination without incorporating any antibiotic resistance marker. Upstream and downstream regions surrounding the gene to be replaced were amplified by overlapping PCR, using Phusion high-fidelity DNA polymerase (Thermo Fisher Scientific). PCR amplification was done in two steps. First, flanking regions of the gene to be eliminated were amplified separately using primers designed to include a NotI restriction site on one end and a complementary tail on the other (Table 2). The resulting upstream and downstream fragments were then used as a template in a second PCR amplification, taking advantage of the overlapping tails present in both amplicons. The resulting product was cloned into a pCR2.1-TOPO vector after adenylation, introduced by transformation into *E. coli* DH5α (56), and sequenced to ensure the absence of mutations. This fragment was then subcloned into the NotI site of pKNG101, a suicide vector unable to replicate in *Pseudomonas* that allows the generation of double-recombination events (57). Plasmid pKNG101 containing the mutation was mobilized from *E. coli* CC118λ*pir* to *P. putida* KT2440 by conjugation, as previously described. Merodiploid exconjugants were selected in minimal medium with citrate and streptomycin. One of these clones was grown in LB medium with 14% sucrose to obtain clones in which a double-recombination event had taken place. Mutants were sucrose resistant and streptomycin sensitive. Null mutants were checked by Southern hybridization and by PCR amplification and sequencing of the corresponding region.

RNA purification and cDNA synthesis. Cultures grown in King's B medium at 30°C for 24 h were centrifuged, the medium was removed, and the pellets were immediately frozen in liquid nitrogen and stored at −80°C until use. Total RNA was extracted using TRI Reagent (Ambion, Austin, TX) according to the manufacturer's protocol, with the exception that the reaction mixture was preheated at 65°C before adding it to the samples, which were incubated for 10 min at 65°C immediately. Samples were treated with RNase-free DNase I (Turbo RNA free; Ambion) plus RNaseOut (Invitrogen), followed by enzyme inactivation with inactivation reagent (Invitrogen). The RNA concentration was determined with a NanoDrop ND1000 spectrophotometer (NanoDrop Technologies, Inc., Wilmington, DE). Sample quality was evaluated through agarose gel electrophoresis, and the absence of residual DNA was checked by PCR. SuperScript II reverse transcriptase (Invitrogen) was used to generate cDNA, with 500 ng of RNA and random hexamers as primers.

qRT-PCR. Quantitative real-time PCR amplifications were performed using iCycler Iq (Bio-Rad, Hercules, CA). The primers used are listed in Table 2. 16S rRNA was used as an internal control for normalization. Each 12.5-μl reaction mixture contained 1 μl of template cDNA and iQ SYBR green Supermix (Bio-Rad). Thermal-cycling conditions were as follows: initial denaturation at 95°C for 10 min,

TABLE 2 Primers used in the study

Primer name	Sequence (5′→3′)[a]	Use
argG-UpF	ATTGCGGCCGCGGTATCGAGCTGGACGCAGC	Null *argG* mutant construction
argG-UpR	**CCGGGGTTTTCGCACACGCCAGCAA**GCCATCACTCCACGGGGTTG	
argG-DwF	**CGTACAACCCCGTGGAGTGATGGC**TTGCTGGCGTGTGCGAAAACC	
argG-DwR	ATTGCGGCCGCTGGCGCGGCGATTTACCAG	
argH-UpF	ATTGCGGCCGCTCGGTCAGCAACTACTACA	Null *argH* mutant construction
argH-UpR	**CGCCACTTTTTCGTTCACGCCTGCA**TCCCCCAAGGCGAGGGCT	
argH-DwF	**AGGGCGAAGCCCTCGCCTTGGGGGA**TGCAGGCGTGAACGAAAAAG	
argH-DwR	ATTGCGGCCGCACATACTTGTGGTCGGCAA	
argF-UpF	ATTGCGGCCGCGTAATTGTGCACGCTCGGGT	Null *argF* mutant construction
argF-UpR	**TTGAGCAGTAGGGGTTGACTCAT**GAGTGACTACCTTATCTGCAAC	
argF-DwF	**CGTTGCAGATAAGGTAGTCACTC**ATGAGTCAACCCCTACTGCTC	
argF-DwR	ATTGCGGCCGCGATGAAACTCGCCACGAATG	
qRTpvdS-F	GCGGAACAACTATCCACAAG	qRT-PCR; *pvdS*
qRTpvdS-R	GAACGATGAGGTGATCTGCG	
qRTpvdA-F	GCACTGTTCATCGACAAGCAG	qRT-PCR; *pvdA*
qRTpvdA-R	GGTGCAGGTAGTTGACGAAG	
qRTpvdE-F	TGCTCAAACCCTTCTGGC	qRT-PCR; *pvdE*
qRTpvdE-R	AGCAGATCGAGCTGAACAG	
qRTpfrA-F	GTTCACAAGCTGATCGACC	qRT-PCR; *pfrA* (=*algQ*)
qRTpfrA-R	GCTCGCAGACTTCGAAGT	
qRTpvdD-F	CTCGATTCCGTGGAGTCAC	qRT-PCR; *pvdD*
qRTpvdD-R	GTCCAGTTGCCAGAGAAAC	
qRTpvdP-F	GTATGTCCAGCGTCAGCTC	qRT-PCR; *pvdP*
qRTpvdP-R	GAACAATTCCAGCGTCTCG	
qRT16S-F	AAAGCCTGATCCAGCCAT	qRT-PCR control; 16S RNA
qRT16S-R	GAAATTCCACCACCCTCTACC	

[a]Restriction sites inserted in the primer for the cloning strategy are underlined. Complementary bases between upstream and downstream fragments of the gene to replace are shown in boldface.

then 40 cycles of amplification (95°C for 10 min; 61°C [for *pfrA*, *pvdS*, *pvdA*, and *pvdP*], 58°C [for *pvdD*], or 56°C [for *pvdE*] for 30 s; and 72°C for 20 s) and a final extension at 72°C for 1 min, with a single fluorescence per reading. The melting curve was obtained by gradually heating the PCR mixture from 55°C to 95°C at a rate of 0.5°C every 10 s for 80 cycles, with continuous fluorescence scanning. Quantification was based on analysis of the threshold cycle (C_T) value (58). Analysis was done using three independent biological replicates, with three technical replicates each.

Detection of siderophore production. To visualize the fluorescence indicative of pyoverdine production in liquid cultures, strains were grown overnight in King's B medium, and the optical density at 660 nm (OD_{660}) was then adjusted to 1 to compare their fluorescences under UV light. Alternatively, the CAS assay was used. CAS-agar plates for siderophore detection were prepared according to the method of Louden and colleagues (59). Plates have a blue color when the dye is complexed with iron(III). The release of siderophore by bacteria and subsequent iron chelation cause a color change, so that an orange halo is produced around colonies. The CAS assay was carried out as follows. Overnight LB cultures were diluted to an OD_{660} of 0.5, and 2-μl drops were spotted in triplicate on CAS-agar plates (square plates containing 30 ml of medium). After incubation at 30°C for 24 h, the halo areas were measured and pictures were taken. Where indicated, solutions of the different compounds at 5 mM final concentration, previously adjusted to pH 6.8, were added to the medium to test their influence upon siderophore production.

Pyoverdine quantification in intracellular/extracellular fractions. Intracellular and extracellular pyoverdine determinations were made as described by Imperi and colleagues (60), with modifications. Cultures of each strain were grown in triplicate in King's B medium in the absence or presence of 5 mM L-arginine for 24 h, and turbidity was measured. Three aliquots of each culture were then taken to obtain extracellular pyoverdine, after centrifugation (9,000 rpm, 5 min, 4°C) to remove bacterial contents. Another three aliquots were used to obtain intracellular pyoverdine as follows: cultures were washed three times with 30 mM Tris-HCl [pH 7], 150 mM NaCl, with centrifuging between washes. Finally, the bacterial pellets were resuspended in 1.2 ml of 10 mM Tris-HCl [pH 8], 100 mM NaCl and lysed by sonication. Cell debris was removed by centrifugation (9,000 rpm, 5 min, 4°C).

Pyoverdine-based fluorescence in extracellular and intracellular fractions was quantified using a Varioskan Lux microplate reader by recording emission at 455 nm upon excitation at 398 nm. Fluorescence readings were corrected for growth (OD_{660}), and average relative values are presented.

Iron determination in culture supernatants. To determine the concentration of iron remaining in the medium after overnight growth, cultures were grown in triplicate in 5 ml liquid King's B medium, and their absorbance (OD_{660}) was measured before centrifugation (9,000 rpm, 5 min, 4°C). Supernatants were collected, and the iron concentration was analyzed by ICP-OES at the Scientific Instrumentation Services of the Estación Experimental del Zaidín.

Oxidative-stress assays. Overnight cultures were diluted to an OD_{660} of 0.05 and grown for 2 h in King's B medium at 30°C with orbital agitation (200 rpm). The cultures were then split in two, one supplied with spermidine at a final concentration of 5 mM and the other with water as a control, and grown for another 30 min before H_2O_2 was added at a final concentration of 5 mM. The cultures were immediately transferred to 96-well microplates (Nunc 96 flat transparent-bottom black polystyrol well plates; Thermo Fisher). Growth (OD_{660}) was monitored every 10 min for 4 h using a Varioskan Lux plate reader (Thermo Fisher).

To determine the oxidative stress of wild-type and mutant strains caused by elevated production or reduced detoxification of ROS in cells during growth, overnight cultures were diluted as described above and grown for 2 h before adding 8 μM CellROX Deep Red reagent 640/665 (Life Technologies). The cultures were incubated for 30 min under the same conditions to allow incorporation of the dye into the cytoplasm and transferred to 96-well microplates (Nunc 96 flat-bottom black polystyrol well plates; Thermo Fisher). Growth (OD_{660}) and fluorescence (excitation at 640 nm and emission at 665 nm) were then monitored every 10 min for 4 h using a Varioskan Lux plate reader (Thermo Fisher). Fluorescence data were normalized with respect to the OD_{660} to correct for potential growth differences.

SUPPLEMENTAL MATERIAL

Supplemental material for this article may be found at https://doi.org/10.1128/JB.00454-19.

SUPPLEMENTAL FILE 1, PDF file, 0.5 MB.

ACKNOWLEDGMENTS

We thank Miryam Rojas for ICP-OES analysis.

This work was funded by grants BFU2016-80122-P from the Plan Estatal de I+D+I and P11-CVI-7391 from Junta de Andalucía and by EFDR funds. L.B.-M. was the recipient of a predoctoral contract from Junta de Andalucía.

REFERENCES

1. Oexle H, Gnaiger E, Weiss G. 1999. Iron-dependent changes in cellular energy metabolism: influence on citric acid cycle and oxidative phosphorylation. Biochim Biophys Acta 1413:99–107. https://doi.org/10.1016/s0005-2728(99)00088-2.
2. Green J, Paget MS. 2004. Bacterial redox sensors. Nat Rev Microbiol 2:954–966. https://doi.org/10.1038/nrmicro1022.
3. Rothery RA, Workun GJ, Weiner JH. 2008. The prokaryotic complex iron-sulfur molybdoenzyme family. Biochim Biophys Acta 1778:1897–1929. https://doi.org/10.1016/j.bbamem.2007.09.002.
4. Puig S, Ramos-Alonso L, Romero AM, Martínez-Pastor MT. 2017. The elemental role of iron in DNA synthesis and repair. Metallomics 9:1483–1500. https://doi.org/10.1039/c7mt00116a.
5. Braun V, Hantke K. 2011. Recent insights into iron import by bacteria. Curr Opin Chem Biol 15:328–334. https://doi.org/10.1016/j.cbpa.2011.01.005.
6. Krewulak KD, Vogel HJ. 2011. TonB or not TonB: is that the question? Biochem Cell Biol 89:87–97. https://doi.org/10.1139/o10-141.
7. Kreamer NN, Wilks JC, Marlow JJ, Coleman ML, Newman DK. 2012. BqsR/BqsS constitute a two-component system that senses extracellular Fe(II) in *Pseudomonas aeruginosa*. J Bacteriol 194:1195–1204. https://doi.org/10.1128/JB.05634-11.
8. Frawley ER, Fang FC. 2014. The ins and outs of bacterial iron metabolism. Mol Microbiol 93:609–616. https://doi.org/10.1111/mmi.12709.
9. Reinhart AA, Oglesby-Sherrouse AG. 2016. Regulation of *Pseudomonas aeruginosa* virulence by distinct iron sources. Genes 7:126. https://doi.org/10.3390/genes7120126.
10. Khan A, Singh P, Srivastava A. 2017. Synthesis, nature and utility of universal iron chelator—siderophore: a review. Microbiol Res 212-213:103–111. https://doi.org/10.1016/j.micres.2017.10.012.
11. Ronnebaum TA, Lamb AL. 2018. Nonribosomal peptides for iron acquisition: pyochelin biosynthesis as a case study. Curr Opin Struct Biol 53:1–11. https://doi.org/10.1016/j.sbi.2018.01.015.
12. Mirleau P, Philippot L, Corberand T, Lemanceau P. 2001. Involvement of nitrate reductase and pyoverdine in competitiveness of *Pseudomonas fluorescens* strain C7R12 in soil. Appl Environ Microbiol 67:2627–2635. https://doi.org/10.1128/AEM.67.6.2627-2635.2001.
13. Ellermann M, Arthur JC. 2017. Siderophore-mediated iron acquisition and modulation of host-bacterial interactions. Free Radic Biol Med 105:68–78. https://doi.org/10.1016/j.freeradbiomed.2016.10.489.
14. Weaver VB, Kolter R. 2004. *Burkholderia* spp. alter *Pseudomonas aeruginosa* physiology through iron sequestration. J Bacteriol 186:2376–2384. https://doi.org/10.1128/jb.186.8.2376-2384.2004.
15. Galet J, Deveau A, Hôtel L, Frey-Klett P, Leblond P, Aigle B. 2015. *Pseudomonas fluorescens* pirates both ferrioxamine and ferricoelichelin siderophores from *Streptomyces ambofaciens*. Appl Environ Microbiol 81:3132–3141. https://doi.org/10.1128/AEM.03520-14.
16. Sexton DJ, Glover RC, Loper JE, Schuster M. 2017. *Pseudomonas protegens* Pf-5 favours self-produced siderophore over free-loading in interspecies competition for iron. Environ Microbiol 19:3514–3525. https://doi.org/10.1111/1462-2920.13836.
17. Halliwell B, Gutteridge J. 1984. Oxygen toxicity, oxygen radicals, transition metals and disease. Biochem J 219:1–14. https://doi.org/10.1042/bj2190001.
18. Touati D. 2000. Iron and oxidative stress in bacteria. Arch Biochem Biophys 373:1–6. https://doi.org/10.1006/abbi.1999.1518.
19. Imlay J. 2015. Transcription factors that defend bacteria against reactive oxygen species. Annu Rev Microbiol 69:93–108. https://doi.org/10.1146/annurev-micro-091014-104322.
20. Kreamer NN, Costa F, Newman DK. 2015. The ferrous iron-responsive BqsRS two-component system activates genes that promote cationic stress tolerance. mBio 6:e02549. https://doi.org/10.1128/mBio.02549-14.
21. Molina MA, Godoy P, Ramos-González MI, Muñoz N, Ramos JL, Espinosa-Urgel M. 2005. Role of iron and the TonB system in colonization of corn

seeds and roots by *Pseudomonas putida* KT2440. Environ Microbiol 7:443–449. https://doi.org/10.1111/j.1462-2920.2005.00720.x.
22. Molina MA, Ramos JL, Espinosa-Urgel M. 2006. A two-partner secretion system is involved in seed and root colonization and iron acquisition by *Pseudomonas putida* KT2440. Environ Microbiol 8:639–647. https://doi.org/10.1111/j.1462-2920.2005.00940.x.
23. Fernández-Piñar R, Cámara M, Soriano MI, Dubern J, Heeb S, Ramos JL, Espinosa-Urgel M. 2011. PpoR, an orphan LuxR-family protein of *Pseudomonas putida* KT2440, modulates competitive fitness and surface motility independently of *N*-acylhomoserine lactones. Environ Microbiol Rep 3:79–85. https://doi.org/10.1111/j.1758-2229.2010.00190.x.
24. Wei H, Aristilde L. 2015. Structural characterization of multiple pyoverdines secreted by two *Pseudomonas* strains using liquid chromatography-high resolution tandem mass spectrometry with varying dissociation energies. Anal Bioanal Chem 407:4629–4638. https://doi.org/10.1007/s00216-015-8659-5.
25. Matilla MA, Ramos JL, Duque E, Alché JD, Espinosa-Urgel M, Ramos-González MI. 2007. Temperature and pyoverdine-mediated iron acquisition control surface motility of *Pseudomonas putida*. Environ Microbiol 9:1842–1850. https://doi.org/10.1111/j.1462-2920.2007.01286.x.
26. Henry PM, Gebben SJ, Tech JJ, Yip JL, Leveau JH. 2016. Inhibition of *Xanthomonas fragariae*, causative agent of angular leaf spot of strawberry, through iron deprivation. Front Microbiol 7:1589. https://doi.org/10.3389/fmicb.2016.01589.
27. Joshi H, Dave R, Venugopalan VP. 2014. Pumping iron to keep fit: modulation of siderophore secretion helps efficient aromatic utilization in *Pseudomonas putida* KT2440. Microbiology 160:1393–1400. https://doi.org/10.1099/mic.0.079277-0.
28. Sasnow SS, Wei H, Aristilde L. 2016. Bypasses in intracellular glucose metabolism in iron-limited *Pseudomonas putida*. MicrobiologyOpen 5:3–20. https://doi.org/10.1002/mbo3.287.
29. Ramos-González MI, Travieso ML, Soriano MI, Matilla MA, Huertas-Rosales Ó, Barrientos-Moreno L, Tagua VG, Espinosa-Urgel M. 2016. Genetic dissection of the regulatory network associated with high c-di-GMP levels in *Pseudomonas putida* KT2440. Front Microbiol 7:1093. https://doi.org/10.3389/fmicb.2016.01093.
30. Jenal U, Reinders A, Lori C. 2017. Cyclic di-GMP: second messenger extraordinaire. Nat Rev Microbiol 15:271–284. https://doi.org/10.1038/nrmicro.2016.190.
31. Schalk IJ, Guillon L. 2013. Pyoverdine biosynthesis and secretion in *Pseudomonas aeruginosa*: implications for metal homeostasis. Environ Microbiol 15:1661–1673. https://doi.org/10.1111/1462-2920.12013.
32. McMorran BJ, Merriman ME, Rombel IT, Lamont IL. 1996. Characterisation of the pvdE gene which is required for pyoverdine synthesis in *Pseudomonas aeruginosa*. Gene 176:55–59. https://doi.org/10.1016/0378-1119(96)00209-0.
33. Yeterian E, Martin LW, Guillon L, Journet L, Lamont IL, Schalk IJ. 2010. Synthesis of the siderophore pyoverdine in *Pseudomonas aeruginosa* involves a periplasmic maturation. Amino Acids 38:1447–1459. https://doi.org/10.1007/s00726-009-0358-0.
34. Nadal-Jimenez P, Koch G, Reis CR, Muntendam R, Raj H, Jeronimus-Stratingh CM, Cool RH, Quax WJ. 2014. PvdP is a tyrosinase that drives maturation of the pyoverdine chromophore in *Pseudomonas aeruginosa*. J Bacteriol 196:2681–2690. https://doi.org/10.1128/JB.01376-13.
35. Leoni L, Orsi N, de Lorenzo V, Visca P. 2000. Functional analysis of PvdS, an iron starvation sigma factor of *Pseudomonas aeruginosa*. J Bacteriol 182:1481–1491. https://doi.org/10.1128/jb.182.6.1481-1491.2000.
36. Tiburzi F, Imperi F, Visca P. 2008. Intracellular levels and activity of PvdS, the major iron starvation sigma factor of *Pseudomonas aeruginosa*. Mol Microbiol 67:213–227. https://doi.org/10.1111/j.1365-2958.2007.06051.x.
37. Venturi V, Otten M, Korse V, Brouwer B, Leong J, Weisbeek P. 1995. Alginate regulatory and biosynthetic gene homologs in *Pseudomonas putida* WCS358: correlation with the siderophore regulatory gene *pfrA*. Gene 155:83–88. https://doi.org/10.1016/0378-1119(94)00868-s.
38. Ambrosi C, Tiburzi F, Imperi F, Putignani L, Visca P. 2005. Involvement of AlgQ in transcriptional regulation of pyoverdine genes in *Pseudomonas aeruginosa* PAO1. J Bacteriol 187:5097–5107. https://doi.org/10.1128/JB.187.15.5097-5107.2005.
39. Rhee HJ, Kim E-J, Lee JK. 2007. Physiological polyamines: simple primordial stress molecules. J Cell Mol Med 11:685–703. https://doi.org/10.1111/j.1582-4934.2007.00077.x.
40. Shah P, Swiatlo E. 2008. A multifaceted role for polyamines in bacterial pathogens. Mol Microbiol 68:4–16. https://doi.org/10.1111/j.1365-2958.2008.06126.x.
41. Friedman ME, Bachrach U. 1966. Inhibition of protein synthesis by spermine in growing cells of *Staphylococcus aureus*. J Bacteriol 92:49–55.
42. Ezekiel DH, Brockman H. 1968. Effect of spermidine treatment on amino acid availability in amino acid-starved *Escherichia coli*. J Mol Biol 31:541–552. https://doi.org/10.1016/0022-2836(68)90426-9.
43. Lal PB, Schneider BL, Vu K, Reitzer L. 2014. The redundant aminotransferases in lysine and arginine synthesis and the extent of aminotransferase redundancy in *Escherichia coli*. Mol Microbiol 94:843–856. https://doi.org/10.1111/mmi.12801.
44. Timmis KN. 2002. *Pseudomonas putida*: a cosmopolitan opportunist *par exellence*. Environ Microbiol 4:779–781. https://doi.org/10.1046/j.1462-2920.2002.00365.x.
45. Visca P, Imperi F, Lamont IL. 2007. Pyoverdine siderophores: from biogenesis to biosignificance. Trends Microbiol 15:22–30. https://doi.org/10.1016/j.tim.2006.11.004.
46. Meyer JM, Gruffaz C, Tulkki T, Izard D. 2007. Taxonomic heterogeneity, as shown by siderotyping, of strains primarily identified as *Pseudomonas putida*. Int J Syst Evol Microbiol 57:2543–2556. https://doi.org/10.1099/ijs.0.65233-0.
47. Xiao R, Kisaalita W. 1998. Fluorescent pseudomonad pyoverdines bind and oxidize ferrous iron. Appl Environ Microbiol 64:1472–1476.
48. Lee J, Sperandio V, Frantz DE, Longgood J, Camilli A, Phillips MA, Michael AJ. 2009. An alternative polyamine biosynthetic pathway is widespread in bacteria and essential for biofilm formation in *Vibrio cholerae*. J Biol Chem 284:9899–9907. https://doi.org/10.1074/jbc.M900110200.
49. Regenhardt D, Heuer H, Heim S, Fernández DU, Strömpl C, Moore ERB, Timmis KN. 2002. Pedigree and taxonomic credentials of *Pseudomonas putida* strain KT2440. Environ Microbiol 4:912–915. https://doi.org/10.1046/j.1462-2920.2002.00368.x.
50. Lennox ES. 1955. Transduction of linked genetic characters of the host by bacteriophage P1. Virology 1:190–206. https://doi.org/10.1016/0042-6822(55)90016-7.
51. Yousef-Coronado F, Travieso ML, Espinosa-Urgel M. 2008. Different, overlapping mechanisms for colonization of abiotic and plant surfaces by *Pseudomonas putida*. FEMS Microbiol Lett 288:118–124. https://doi.org/10.1111/j.1574-6968.2008.01339.x.
52. King EO, Ward MK, Raney DE. 1954. Two simple media for the demonstration of pyocyanin and fluorescin. J Lab Clin Med 44:301–307.
53. Ausubel FM, Brent R, Kingston RE, Moore DD, Seidman JG, Smith JA, Struhl K. 1987. Current protocols in molecular biology. Wiley, New York, NY.
54. Sambrook J, Russell DW. 2001. Molecular cloning: a laboratory manual. Cold Spring Harbor Laboratory Press, Cold Spring Harbor, NY.
55. Herrero M, de Lorenzo V, Timmis KN. 1990. Transposon vectors containing non-antibiotic resistance selection markers for cloning and stable chromosomal insertion of foreign genes in gram-negative bacteria. J Bacteriol 172:6557–6567. https://doi.org/10.1128/jb.172.11.6557-6567.1990.
56. Woodcock DM, Crowther PJ, Doherty J, Jefferson S, DeCruz E, Noyer-Weidner M, Smith SS, Michael MZ, Graham MW. 1989. Quantitative evaluation of *Escherichia coli* host strains for tolerance to cytosine methylation in plasmid and phage recombinants. Nucleic Acids Res 17:3469–3478. https://doi.org/10.1093/nar/17.9.3469.
57. Kaniga K, Delor I, Cornelis GR. 1991. A wide-host-range suicide vector for improving reverse genetics in Gram-negative bacteria: inactivation of the *blaA* gene of *Yersinia enterocolitica*. Gene 109:137–141. https://doi.org/10.1016/0378-1119(91)90599-7.
58. Pfaffl MW. 2001. A new mathematical model for relative quantification in real-time RT-PCR. Nucleic Acids Res 29:e45. https://doi.org/10.1093/nar/29.9.e45.
59. Louden BC, Haarmann D, Lynne AM. 2011. Use of blue agar CAS assay for siderophore detection. J Microbiol Biol Educ 12:51–53. https://doi.org/10.1128/jmbe.v12i1.249.
60. Imperi F, Tiburzi F, Visca P. 2009. Molecular basis of pyoverdine siderophore recycling in *Pseudomonas aeruginosa*. Proc Natl Acad Sci U S A 106:20440–20445. https://doi.org/10.1073/pnas.0908760106.